Imaging of Diffuse and Inflammatory Liver Disease

22

Pablo R. Ros

Learning Objectives

- To describe the pathophysiology of common and unusual diffuse diseases of the liver
- To learn to differentiate the overstorage of fat, iron, copper, and amyloid in the liver based on cross-sectional imaging
- To review diffuse hepatic manifestations of extrahepatic neoplasms
- To illustrate typical imaging findings of diffuse and focal liver infections including fungal, viral, parasitic, and bacterial etiology

22.1 Introduction

The role of imaging in the detection, characterization, and follow-up of diffuse liver disease has increased due to advances in cross-sectional imaging.

Diffuse liver disease is classified classically along pathogenesis into cirrhosis, vascular diseases, congenital, metabolic and storage, and neoplastic [1–5]. This chapter discusses the last three categories and in addition includes both diffuse and focal inflammatory/infectious diseases. Elsewhere in this syllabus, cirrhosis and vascular diseases are reviewed.

P. R. Ros
Department of Radiology, University Hospitals Health System/
Case Western Reserve University, Cleveland, OH, USA
e-mail: Pablo.Ros@UHhospitals.org

22.2 Metabolic and Storage Diseases

22.2.1 Steatosis and Steatohepatitis

Hepatic steatosis results from a variety of abnormal processes including increased production or mobilization of fatty acids (e.g., obesity, steroid use) or decreased hepatic clearance of fatty acids due to hepatocellular injury (e.g., alcoholic liver disease, viral hepatitis). Histopathologically, the hallmark of all forms of fatty liver is the accumulation of fat globules within the hepatocytes. The distribution of steatosis can be variable, ranging from focal, to regional, to diffuse. Diffuse steatosis is common and estimated to occur in approximately 30% of obese patients. Patients with steatosis are usually asymptomatic although some individuals may present with right upper quadrant pain or abnormal liver function parameters. Non-alcohol-related liver steatosis is also known as nonalcoholic fatty liver disease (NAFLD). Histopathologic findings of NAFLD vary from steatosis alone to steatosis with inflammation, necrosis, and fibrosis. At the most severe end of the NAFLD spectrum resides nonalcoholic steatohepatitis (NASH), with or without cirrhosis. Histopathologic findings of NASH include steatosis (predominately macrovesicular), mixed lobular inflammation, and hepatocellular ballooning. Unlike steatosis alone, NASH may progress to cirrhosis.

CT easily identifies diffuse steatosis. The attenuation value of normal liver is usually on average 8 HU greater than that of spleen on non-contrast CT images. In patients with fatty change, however, an abnormally decreased density will be demonstrated, typically 10 and 25 HU less than the spleen on non-contrast CT and contrast-enhanced CT images, respectively. The diagnosis of hepatic steatosis is more reliably made on non-contrast images.

© The Author(s) 2018
J. Hodler et al. (eds.), *Diseases of the Abdomen and Pelvis 2018–2021*, IDKD Springer Series,
https://doi.org/10.1007/978-3-319-75019-4_22

Key Points

- The extent of fatty changes, iron deposition, and fibrotic remodeling can be quantified using MRI although their simultaneous presence can influence each other's results.
- Metastatic liver disease demonstrates mostly a multifocal disease, diffuse, and subtle presentation, requiring awareness and interpretation of indirect features.
- The liver is one of the most affected organs in parasitic diseases. Radiologists should be able to recognize and suspect the most relevant parasitic diseases, including hepatic schistosomiasis and echinococcosis.
- Acute hepatitis results in increased T1 and T2 relaxation times as well as periportal edema. Chronic hepatitis doesn't necessarily show distinct imaging features before developing into cirrhotic changes at long term.
- Imaging in infectious diseases might be crucial as they can be fatal if not promptly treated. With the help of CT and MRI, entities that may manifest with similar clinical and laboratory findings can be excluded.

Undoubtedly the most sensitive technique to detect fatty change of the liver is the use of inphase and out-of-phase gradient echo MR pulse sequences (Fig. 22.1). Multi-echo sequences, MR spectroscopy, and other MR techniques have been proposed to quantify the fat burden in the liver with success. Conjoint iron deposition, however, may be a confounding factor in estimating the fat fraction based on dual-echo chemical shift imaging. The fat fraction may be overestimated, and, therefore, the component of iron deposition requires correction as suggested by Kang et al.

Hepatic fatty change is, however, not always uniform but can present as a focal area of steatosis in an otherwise normal liver (focal steatosis) or as subtotal fatty change with sparing of certain areas (focal sparing) (Fig. 22.2). On imaging, several features allow the correct identification of focal fatty change or focal spared areas: (1) the typical periligamentous and periportal location, (2) lack of mass effect, (3) sharply angulated boundaries of the area, (4) nonspherical shape, (5) absence of vascular displacement or distorsion, and (6) lobar or segmental distribution [6, 7].

22.2.2 Iron Overload

Iron overload states are categorized in hemochromatosis, where the iron accumulates preferentially within the hepatocytes, and hemosiderosis, where it is deposited in the Kupffer cells.

22.2.2.1 Primary Hemochromatosis

Hereditary or primary hemochromatosis is an autosomal recessive disorder of iron metabolism characterized by abnormal absorption of iron from the gut with subsequent excessive deposition of iron into the hepatocytes, pancreatic acinar cells, myocardium, joints, endocrine glands, and skin. In addition, the reticuloendothelial system (RES) cells in patients with primary hemochromatosis are abnormal and unable to store processed iron effectively. As a consequence, patients with primary hemochromatosis don't accumulate iron into the RES. Clinical findings of cirrhosis and its complications (portal hypertension, development of HCC) predominate in patients with long-lasting disease.

On CT excessive storage of iron into the hepatocytes will result in an overall *increased* density. However, this CT appearance of a hyperdense liver is nonspecific since similar features can be seen with gold deposition and in Wilson's disease, type IV glycogen storage disease, and following amiodarone administration. Performing non-contrast CT in patients with suspected hemochromatosis is important because excessive iron cannot be detected in the setting of enhancing parenchyma. However, the sensitivity of CT for iron is often insufficient as there is.

(a) A minimum threshold for liver iron detection that is five times higher than the normal liver iron level.
(b) Concomitant liver steatosis (hypodense appearance) may be similar to the CT appearance of early iron overstorage.

MRI is far more specific than any other imaging modalities for the characterization of iron overload due to the paramagnetic properties of iron. The superparamagnetic effect of accumulated iron in the hepatocytes results in significant reduction of T2 or T2* relaxation times which diminish the signal intensity on T2-weighted or on T1-weighted multi-echo spoiled gradient-echo images. Conversely to excessive storage of fat, in iron deposition, there will be an increase of signal intensity in chemical shift imaging from the in phase to the opposed phase. The amount of iron can be quantified using gradient-echo sequences with T2* weighting and progressively longer echo times. In general, comparison of the signal intensity of liver with that of paraspinal muscles provides a useful internal control. Hepatocellular carcinomas, complicating 35% of patients with advanced hemochromatosis, are usually easily detected on both T1- and T2-weighted images due to the background of decreased signal intensity of the liver [8, 9].

22.2.2.2 Hemosiderosis

In patients with hemosiderosis or siderosis, either due to transfusional iron overload states or dyserythropoiesis (e.g., thalassemia major, sideroblastic anemia, pyruvate kinase deficiency, chronic liver disease), the excessive iron is

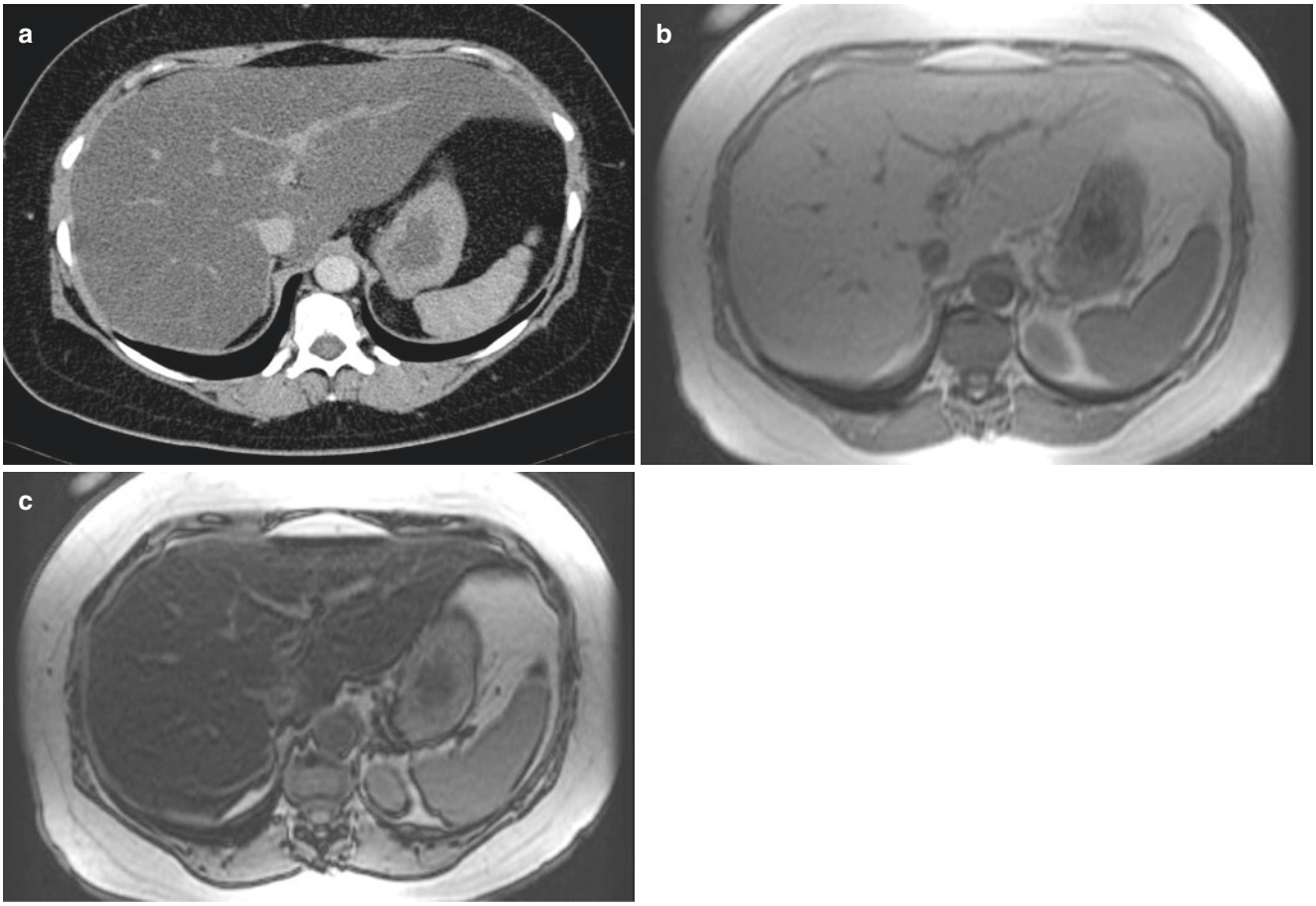

Fig. 22.1 Diffuse fatty liver. 41-year-old female presenting with epigastric pain. Axial CECT image (**a**) demonstrates diffuse low attenuation of the liver without displacement of the hepatic vessels. In- (**b**) and out-of-phase (**c**) T1-weighted new MRI images show significant signal drop in the liver on the out-of-phase images

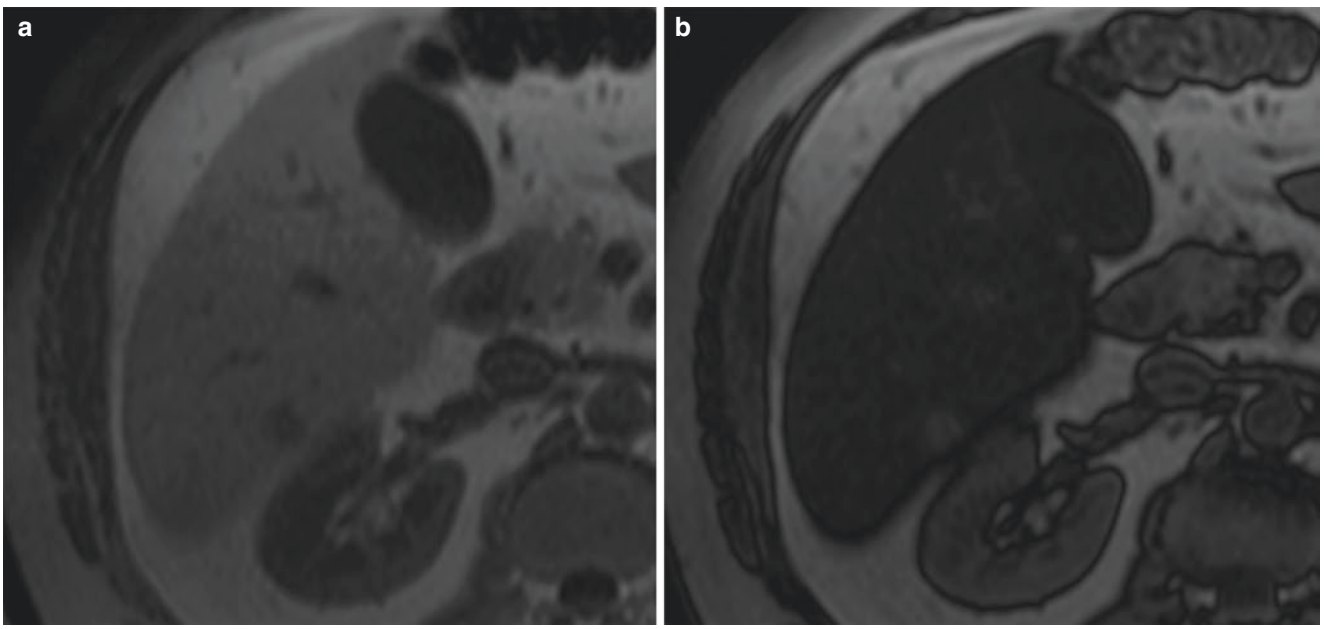

Fig. 22.2 Hemosiderosis. Focal fatty sparing. 59-year-old male with right upper quadrant pain and elevated liver function tests. Axial chemical shift MRI images show signal drop of the entire steatotic liver from in- (**a**) to out-of-phase (**b**) with focal fatty sparing in liver segment 6

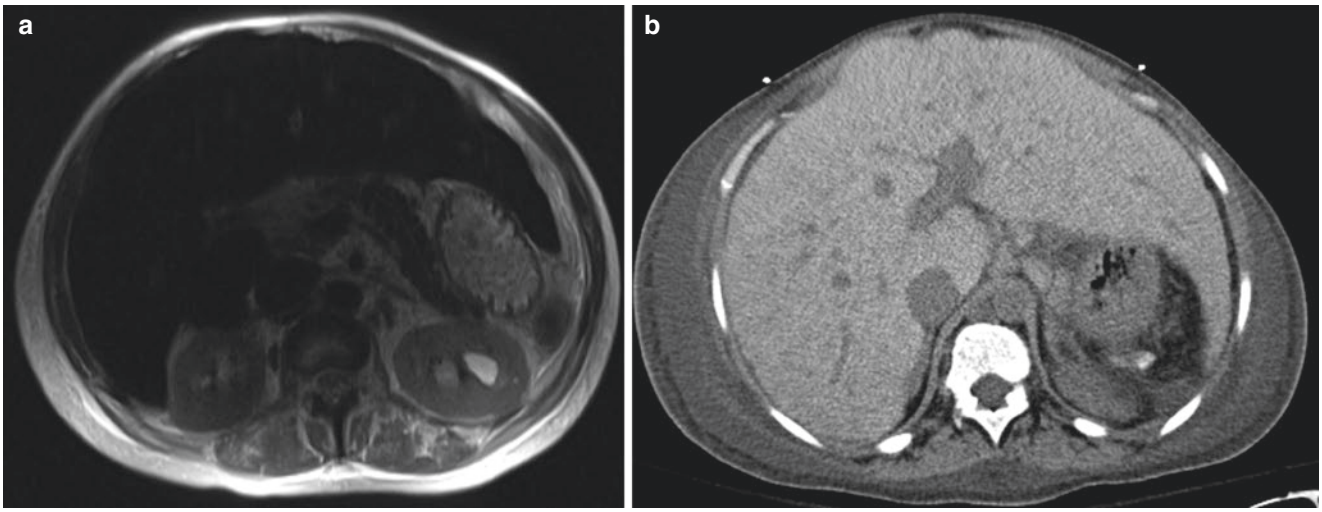

Fig. 22.3 29-year-old female with long history of sickle cell anemia requiring multiple transfusions. Axial T2-weighted MRI demonstrates significantly decreased liver-signal intensity and NECT increased attenuation in the liver due to the iron overload

processed and accumulates in organs containing reticuloendothelial cells, including liver, spleen, and bone marrow.

By CT, there is diffuse, increased attenuation of liver and spleen (Fig. 22.3). In MRI, the extrahepatic signal intensity changes in the spleen and bone marrow allow MR imaging to distinguish primary hemochromatosis from hemosiderosis. Although in general the clinical significance of transfusional iron overload states is negligible, patients with chronic hemosiderosis can develop symptoms similar to those of the primary form as well as cirrhosis and HCC.

22.2.3 Wilson Disease

Wilson disease, also known as hepatolenticular degeneration, is a rare autosomal recessive abnormality of copper metabolism characterized by accumulation of toxic levels of copper in the brain, cornea (Kayser-Fleischer rings), and liver, the latter due to impaired biliary excretion. Hepatic deposition of copper, predominantly seen in periportal areas and along the hepatic sinusoids, evokes an inflammatory reaction resulting in acute hepatitis with fatty change. Subsequently, chronic hepatitis may result in liver fibrosis and eventually macronodular cirrhosis.

Due to the high atomic number of copper, a hyperdense liver may be seen on unenhanced CT scans. However, this finding is not universally present, and usually only nonspecific signs such as hepatomegaly, fatty change, and, in advanced cases, cirrhosis are observed. During the early stage of the disease due to the paramagnetism of ionic copper, MR imaging can be valuable by demonstrating focal copper depositions as multiple nodular lesions, typically appearing hyperintense and hypointense on T1- and T2-weighted images, respectively, as described by Cheon JE et al [10].

22.2.4 Amyloidosis

Amyloidosis consists of deposition of fibrils of protein-mucopolysaccharide complexes throughout the body and is classified based on the biochemical composition of the amyloid fibrils. Primary amyloidosis is due to the deposition of immunoglobulin light chains and is associated with multiple myeloma and monoclonal gammopathy. Secondary amyloidosis is due to deposition of amyloid A protein and is associated with chronic infection, rheumatoid arthritis, and malignancies. Exceeded only by the spleen and kidney, the liver is the third most common solid organ prone to this deposition.

Hepatic amyloidosis has a nonspecific imaging appearance. The most common finding is diffuse hepatomegaly. CT sporadically demonstrates focal areas of low attenuation within the liver corresponding to sites of amyloid deposition (amyloid pseudotumor). Patients may present with a picture of jaundice which is due to intrahepatic cholestasis [11, 12].

22.3 Neoplastic Diseases

22.3.1 Metastatic Disease

Neoplastic infiltration due to diffuse metastatic disease can occur with many primary tumors. Melanoma, malignant neuroendocrine tumors, pancreatic adenocarcinoma, breast carcinoma, and colonic adenocarcinoma are some of the more commonly encountered causes of diffuse hepatic metastatic disease.

CT appearances of hepatic metastases depend on the vascularity of the lesions compared with the normal liver parenchyma. Diffuse metastatic involvement may produce only subtle imaging findings and be only detectable through

Fig. 22.4 Diffuse metastatic breast cancer (pseudocirrhosis pattern). 43-year-old female treated for metastatic breast cancer. Axial CECT image demonstrates several small low-density lesions in the liver and a nodular contour of the liver due to hepatic capsular retraction

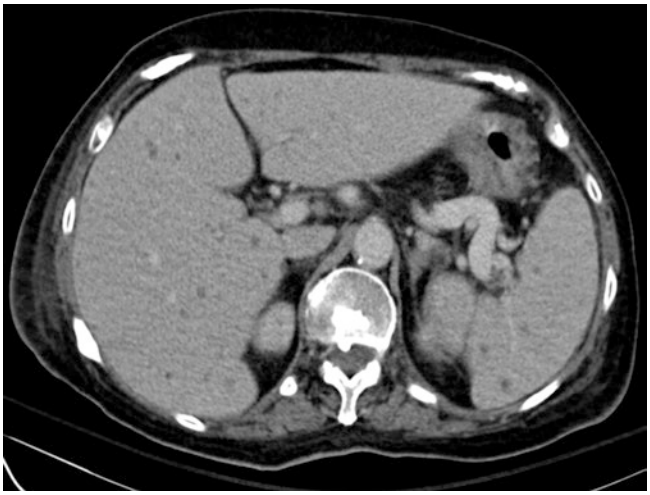

Fig. 22.5 Hepatic candidiasis. 66-year-old female with leukemia presenting with abnormal liver function tests. Axial CECT image demonstrates multiple small low-attenuation lesions seen throughout the liver and spleen. Splenomegaly and bilateral pleural effusions are also present

indirect features, such as diffuse parenchymal heterogeneity, vascular and architectural distortion, or alterations of the liver contour. The latter, particularly seen in patients with treated breast cancer metastases, has been reported as the "pseudocirrhosis" sign (Fig. 22.4). In addition, treated breast cancer metastases may mimic the appearance of liver hemangiomata.

22.3.2 Lymphoma

Lymphoma can infiltrate the liver both primarily and secondarily. Primary lymphoma of the liver is extremely rare. Conversely the liver is often secondarily involved in both Hodgkin's and non-Hodgkin's lymphoma. Typically, the liver parenchyma is diffusely infiltrated with microscopic nests of neoplastic cells without significant architectural distortion, and, therefore, lymphomatous involvement is difficult to detect by imaging alone. Associated abnormalities, such as splenomegaly and lymphadenopathy, may narrow the differential diagnosis.

22.4 Diffuse Infectious and Inflammatory Diseases

22.4.1 Fungal Infections

Hepatosplenic fungal infection is a clinical manifestation of disseminated fungal disease in patients with hematologic malignancies or compromise of the immunologic system. The reported prevalence of fungal dissemination ranges from 20% to 40%. Most hepatic fungal microabscesses occur in leukemia patients and are caused by *Candida albicans* [16].

22.4.1.1 Candidiasis

Candida albicans, in the liver, may evoke little or no inflammatory reaction, cause a superlative response, or occasionally produce granulomas. The typical histologic pattern of hepatic candidiasis is characterized by microabscesses, with the yeast or pseudohyphal forms of the fungus in the center of the lesion and a surrounding area of necrosis and polymorphonuclear infiltrate.

At contrast-enhanced CT, fungal microabscesses usually appear as multiple rounds, discrete areas of low attenuation, generally ranging from 2 to 20 mm (Fig. 22.5). These microabscesses usually enhance centrally after intravenous administration of contrast medium, although peripheral enhancement may occur.

At MR imaging, the untreated nodules are rounded lesions less than 1 cm in diameter that are minimally hypointense on T1-weighted and gadolinium-enhanced images and markedly hyperintense on T2-weighted images. After treatment, lesions appear mildly to moderately hyperintense on T1- and T2-weighted images and demonstrate enhancement on gadolinium-enhanced images. A dark ring is usually seen around these lesions with all sequences. Completely treated lesions are minimally hypointense on T1-weighted images, isointense to mildly hyperintense on T2-weighted images, moderately hypointense on early gadolinium-enhanced images, and minimally hypointense on delayed gadolinium-enhanced images. MR imaging is superior to CT and US in the detection of these fungal foci [17].

22.4.2 Granulomatous Diseases

Granulomatous hepatitis is associated with a wide variety of conditions, most commonly with sarcoidosis, tuberculosis, and histoplasmosis. Hepatic granulomas usually appear as discrete, sharply defined nodules consisting of aggregates of epithelioid cells by a rim of mononuclear cells, predominantly lymphocytes.

22.4.2.1 Sarcoidosis

Sarcoidosis is a multisystem disorder of unknown pathogenesis, characterized by noncaseating granulomas. Although it may involve almost any organ in the body, pulmonary sarcoidosis is most common. Sarcoidosis of the liver is also relatively frequently seen, but the granulomas are usually not macroscopically detectable and thus may not produce focal abnormalities on imaging studies. Classically, the granulomas develop in a periportal location resulting in periportal fibrosis, cirrhosis, and eventually portal hypertension.

Hepatic contrast-enhanced CT may typically reveal multiple, diffuse small low-density areas in both the liver and spleen (Fig. 22.6). MRI features of hepatic sarcoidosis are also nonspecific and include organomegaly, multiple low-signal-intensity lesions relative to background parenchyma with all sequences, increased periportal signal, irregularity of the portal and hepatic vein branches, and patchy areas of heterogeneous signal. Recent literature by Ferreira et al. confirms the nonspecific appearance but describes as a characteristic feature with large central regenerative nodules and wedge-shaped areas of peripheral parenchymal atrophy [18, 19].

22.4.2.2 Tuberculosis

Tuberculosis is one of the most common infectious diseases worldwide. Generally, tuberculosis in the liver presents as either miliary or focal form. Focal hepatic TB is further subdivided into nodular (i.e., tuberculous abscess and tuberculoma) and tubular or hepatobiliary tuberculosis (i.e., tuberculosis involving the intrahepatic ducts). Hepatic miliary tuberculosis is the most common and is reported to occur in 50–80% of all patients with terminal pulmonary tuberculosis. Miliary tuberculosis is usually not detected by imaging. Hepatomegaly may be the only radiological abnormality.

In the healing stage of tuberculosis, CT may show diffuse hepatic calcifications (approximately 50% of cases). Reported CT findings of nodular tuberculosis are nonspecific and include hypoattenuating lesions both before and after intravenous contrast administration.

At MR imaging, the lesions are hypointense on T1-weighted images and hypo- to isointense on T2-weighted images. Tuberculosis lesion differently enhances after gadolinium administration. Because of these rather nonspecific findings with all imaging techniques, percutaneous liver biopsy is necessary [20].

22.4.2.3 Histoplasmosis

Histoplasmosis is the most common cause of fungal infection in the Ohio River Valley of the United States. Fortunately, 99% of patients exposed to histoplasmosis develop only subclinical infections. Liver involvement is common in disseminated histoplasmosis, which usually originates in the lungs. The most common hepatic findings include portal lymphohistiocytic inflammation and discrete, well-delineated granu-

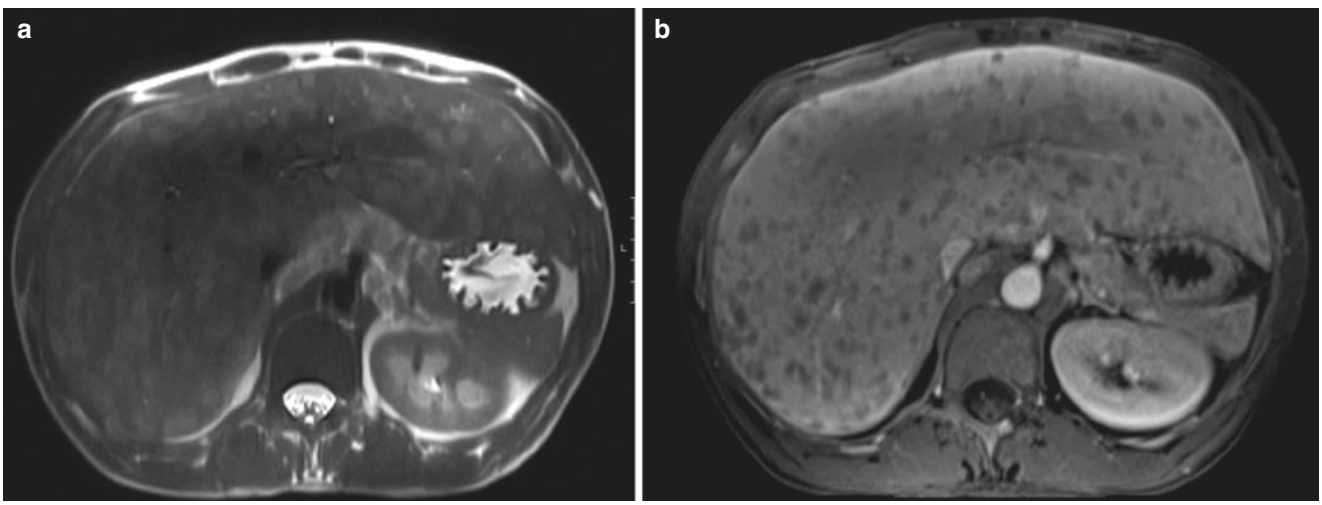

Fig. 22.6 Hepatic sarcoidosis. 44-year-old male with fever and hilar adenopathy on chest X-ray. Axial T2-weighted (left) and T1-weighted post-contrast (right) MR images show multiple small T2-hyperintense, T1-hypointense, ring-enhancing lesions throughout the liver. Note the small spleen that is consistent with chronic auto infarction from coexisting sickle cell anemia

lomas. In patients with healed histoplasmosis, the presence of small, punctate calcifications scattered throughout the liver and spleen is typical but nonspecific finding [21].

22.4.3 Parasitic Infections

22.4.3.1 Schistosomiasis

Schistosoma japonicum, *S. haematobium*, and *S. mansoni* are the three most important species that infect humans. The schistosomas live in the bowel lumen and lay eggs in the mesenteric veins. The eggs may then embolize to the portal vein. The eggs themselves do not survive and subsequently calcify. Chronic infections with either *S. japonicum* or *S. mansoni* result in the formation of cirrhosis and the risk of development of hepatocellular carcinoma. Histologically, schistosomiasis is characterized by white, pinhead-sized granulomas scattered throughout the liver. At the center of each granuloma is a schistosome egg. Periportal fibrosis is the major pathological consequence of the *Schistosoma mansoni* infection. In severe infections, the surface of the liver shows granulomatous involvement and widespread fibrous portal enlargement ("pipestem" fibrosis).

At CT, the most pathognomonic pattern is the presence of calcified septa, usually aligned perpendicular to the liver capsule ("tortoiseshell" or "turtleback" appearance).

22.4.4 Viral Infections

22.4.4.1 Viral Hepatitis

Acute viral hepatitis is a systemic infection that affects the liver and is usually caused by one of five viral agents: hepatitis A virus, hepatitis B virus (HBV), hepatitis C virus, the HBV-associated delta agent or hepatitis D virus, and hepatitis E virus. A vast array of other viruses may also produce hepatitis, including herpes viruses, yellow-fever virus, rubella virus, Coxsackievirus, and adenovirus. The diagnosis of acute hepatitis is usually based on serologic, virologic, and clinical findings. Probably the most important role of radiology in patients with acute hepatitis is to help rule out other diseases that produce similar clinical and biochemical abnormalities, such as extrahepatic cholestasis, diffuse metastatic disease, and cirrhosis.

At CT and MR imaging, findings in acute viral hepatitis are nonspecific and include hepatomegaly and periportal edema. At CT, heterogeneous enhancement and well-defined regions of low attenuation may be present. At MR imaging, periportal edema appears as high-signal-intensity areas on T2-weighted images. Involved areas may be normal or demonstrate decreased signal intensity on T1-weighted images and increased signal intensity on T2-weighted images. There is also impaired uptake of liver-specific agents. Extrahepatic findings in patients with severe acute hepatitis include gallbladder wall thickening due to edema and, infrequently, ascites. In chronic hepatitis, the CT and MR imaging features resemble those of early-stage liver cirrhosis. Periportal lymphadenopathy may be the sole detectable abnormality in both acute and chronic hepatitis.

22.4.4.2 HIV Infection

The liver and biliary tracts are frequent sites of involvement during the course of HIV infection. Coinfection with hepatitis B and C viruses is particularly common due to the shared means of transmission of these viruses with HIV. AIDS-related cholangiopathy is the newest common manifestation. At CT, inflammation of the gallbladder or biliary tree manifests as mural thickening or abnormal contrast enhancement. MRCP is more sensitive and specific than US or CT in depicting the mural irregularity of the extrahepatic ducts that result from the exuberant periductal inflammation, focal mucosal ulcers, and interstitial edema found in AIDS-related cholangitis.

22.4.5 Uncommon Hepatic Infections

22.4.5.1 Cat-Scratch Disease

Cat-scratch disease is an infection that affects immunocompetent children or adolescents. It is caused by *Bartonella henselae*, a gram-negative bacillus that is usually introduced by the scratch of a cat. Cat-scratch disease takes many forms, from regional lymphadenitis to disseminated infection. The typical clinical manifestation of cat-scratch disease is painful lymphadenopathy proximal to the site of inoculation. Disseminated infection is seen in 5–10% of cases. In the abdomen, multiple granulomas ranging from 3 to 30 mm may form in the liver and spleen, with or without hepatosplenomegaly. Histopathologic findings include vascular proliferative lesions (peliosis hepatis) and necrotizing granulomatous lesions.

At unenhanced CT, the lesions are hypoattenuating relative to normal parenchyma. Three different patterns at contrast-enhanced CT have been described: *(a)* persistent hypoattenuation relative to the liver, *(b)* isoattenuation relative to surrounding tissues, and *(c)* marginal enhancement. Only a few MR imaging studies of cat-scratch disease have been described. The lesions appear as low-signal-intensity nodules on T1-weighted MR images and as high-signal-intensity nodules on T2-weighted images. Peripheral enhancement may be seen on gadolinium-enhanced T1-weighted images [23, 24].

22.4.5.2 Bacillary Angiomatosis

Bacillary angiomatosis is also a manifestation of infection by *Bartonella henselae in* immunocompromised patients.

This is the same organism that causes cat-scratch disease in noncompromised patients. It is characterized by localized areas of vascular proliferation that may affect the skin, airway, mucous membranes, visceral organs, bone, and brain. Contrast-enhanced CT may demonstrate multiple diffuse low- or high-attenuation lesions less than 1 cm scattered throughout the hepatic parenchyma. Ascites, mild periportal edema, and intrahepatic biliary ductal dilatation may occur. These imaging features are nonspecific and must be distinguished, especially in AIDS patients, from hepatic abscesses related to other bacteria, viruses, or fungi; AIDS-related lymphoma; Kaposi sarcoma; and, less commonly, disseminated *Pneumocystis carinii* infection [25].

22.5 Focal Infections

22.5.1 Bacterial (Pyogenic) Abscess

Pyogenic abscess, although uncommon in the antibiotic era, is still challenging clinically since its presentation is quite variable, from profound septicemia to chronic, indolent symptoms.

Enhanced CT can reliably diagnose over 90% of hepatic pyogenic abscesses, revealing two main patterns: multiple microabscesses (disseminated or clustered) and large macroabscesses. By virtue of its good spatial and contrast resolution, computed tomography (CT) is the single best method for detecting hepatic abscess, with a sensitivity as high as 97%. On CT scans, abscesses appear as generally rounded masses that are hypodense on both contrast and non-contrast scans. Central gas, either as air bubbles or an air-fluid level, is a specific sign, but it is present in less than 20% of cases. A thick, enhancing, peripheral rim is also noted.

At MR imaging, air within the abscess appears as a signal void and is therefore more difficult to differentiate from calcifications. However, the shape and location (air-fluid level) should enable the correct diagnosis. After administration of gadolinium-DTPA, abscesses typically show rim enhancement (the "double-target" sign). Small lesions (<1 cm) may enhance homogeneously mimicking hemangiomas. Percutaneous, image-guided aspiration followed by drainage is the method of choice for definitive diagnosis and treatment with success in over 90% of cases.

22.5.2 Amebic Abscess

Hepatic abscess is the most common extraintestinal manifestation of amebiasis, affecting approximately 10% of patients with amebiasis. Although rare in the continental United States, 10% of the world's population is infected with *Entamoeba histolytica*. Clinically, patients with amebic abscess are more acutely ill than patients with pyogenic abscess, with high fever and right upper quadrant pain. Diagnosis is made by positive serologic amebic titers, although they have false-negative rates of almost 20%.

CT demonstrates well the extrahepatic extensions to chest wall, pleura, or adjacent viscera. Percutaneous catheter drainage of an amebic abscess is rarely necessary because of the effectiveness of amebicidal therapy. Occasionally, percutaneous drainage is needed in large, symptomatic abscesses with poor response to medical therapy, suspected bacterial superinfection, and threatening intrapericardial rupture. The CT appearance of amebic abscess is variable and nonspecific. The lesions are usually peripheral, round, or oval areas of low attenuation (10–20 Hounsfield units). A peripheral rim of slightly higher attenuation can be seen on non-contrast scans and shows marked enhancement after administration of contrast material.

On MR imaging, amebic liver abscesses are spherical and usually solitary lesions with a hyperintense center on T2-weighted images and a hypointense center on T1-weighted images. The abscess wall is thick, and on gadolinium-enhanced images, the enhancement pattern is similar to that of pyogenic abscess [26].

22.5.3 Echinococcal Disease

Hydatid disease has two main forms affecting humans *Echinococcus granulosus* and *Echinococcus multilocularis or alveolaris*. These infections have well-defined and different geographic distributions. The pathologic and imaging findings differ dramatically between these parasites.

On CT scans, *E. granulosus* appears as unilocular or multilocular, well-defined cysts with either thick or thin walls. Daughter cysts are usually seen as areas of lower attenuation than the mother cyst and are usually in the periphery of the lesion. Daughter cysts can also float free in the lumen of the mother cyst, so altering the patient's position may change the position of these cysts, confirming the diagnosis of echinococcal disease. Curvilinear ring-like calcification is also a common feature.

On MR studies, the cyst component of echinococcal cysts is similar to that of other cysts, with long T1 and T2 relaxation times. However, MR imaging best demonstrates the pericyst, the matrix and hydatid sand (debris consisting of freed scolices), and the daughter cysts. The pericyst usually has low-signal intensity on T1- and T2-weighted images, because of its fibrous component. This rim and a multiloculated or multicystic appearance are distinctive features. The

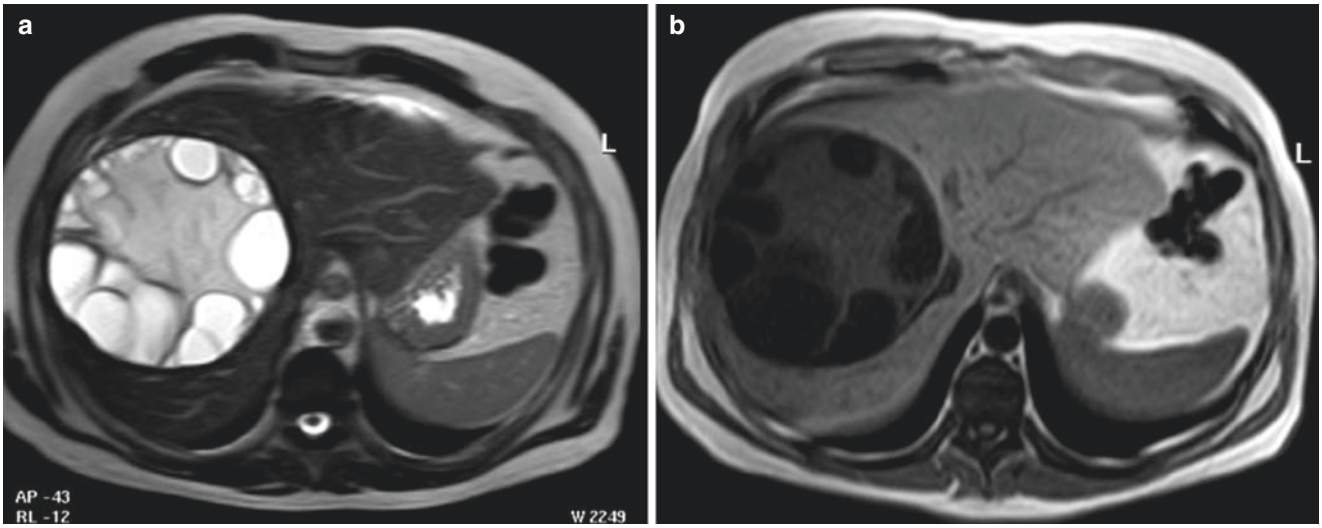

Fig. 22.7 Echinococcus granulosus cyst. 28-year-old man with right upper quadrant pain. Axial (**a**) T2-weighted image demonstrates a large cystic mass in the right lobe of the liver which is surrounded by a hypointense rim and contains more hyperintense smaller cysts in its periphery. On the axial T1-weighted image (**b**), the hypointense rim is well visualized, and the peripheral cysts are hypointense relative to the center of the lesion

hydatid matrix appears hypointense on T1-weighted images and markedly hyperintense on T2-weighted images. When present, daughter cysts are hypointense relative to the matrix on both T1- and T2-weighted images (Fig. 22.7). Floating membranes have low-signal intensities on T1- and T2-weighted images.

E. multilocularis appears as a solid large mass or masses, with minimal to no enhancement after intravenous administration of contrast material and possible small punctate calcification [27–29].

22.6 Concluding Remarks

The spectrum of diffuse liver diseases includes a broad range of different entities including metabolic, storage, neoplastic, infectious, and inflammatory disorders. They may have unique or overlapping image findings. Knowing the typical features of the different diffuse and inflammatory liver diseases with CT and MRI techniques allows radiologists to play a key role in the diagnosis and management of diffuse liver diseases. Likewise, focal inflammatory diseases such as abscesses and hydatid disease can be characterized by imaging [14, 22, 30].

Acknowledgments We appreciate the contributions of Verena Obmann, MD, in updating this manuscript from it's prior version (cite: Hodler J, Kubik-Huch R, von Schulthess GK, Zollikofer ChL, editors. Diseases of the abdomen and pelvis 2014–2017. Springer 2014. pp. 87–94).

Take-Home Messages

- Storage diseases generally involve the liver diffusely but can also manifest as focal alterations and can mimic other pathologies including malignancy.
- Diffuse neoplastic involvement may produce subtle imaging findings and be only detectable through indirect features, such as hepatomegaly, diffuse parenchymal heterogeneity, vascular and architectural distortion, or alterations of the liver contour.
- Imaging in infectious diseases might be crucial as they can be fatal if not promptly treated. CT and MRI play a crucial role to differentiate and characterize diffuse and inflammatory liver disease.

References

1. Hamm B, Ros PR, editors. Abdominal imaging, vol. 1–4. Berlin: Springer; 2013.
2. Ros PR, Mortele KJ, Pelsser V, Thomas S. CT/MRI of the abdomen and pelvis: a teaching file. 3rd ed. Philadelphia, PA: Wolters Klumer/Lippincott, Williams and Wilkins; 2013.
3. Ros PR. Hepatic imaging and intervention. In clinics in liver disease. Philadelphia, PA: W.B. Saunders; 2002.
4. Mortele KJ, Ros PR. Imaging of diffuse liver disease. Semin Liver Dis. 2001;21(2):195–212.
5. Chundru S, Kalb B, Arif-Tiwari H, Sharma P, Costello J, Martin DR. MRI of diffuse liver disease: the common and uncommon etiologies. Diagn Interv Radiol. 2013;19(6):479–87.

6. Other GB. Diffuse liver diseases: steatosis, hemochromaosis, etc. In: Hamm B, Ros PR, editors. Abdominal imaging, vol. 70. Berlin: Springer; 2013. p. 1027–44. Volume II Sec. V.
7. Kang BK, Yu ES, Lee SS, Lee Y, Kim N, Sirlin CB, Cho EY, Yeom SK, Byun JH, Park SH, Lee MG. Hepatic fat quantification: a prospective comparison of magnetic resonance spectroscopy and analysis methods for chemical-shift gradient echo magnetic resonance imaging with histologic assessment as the reference standard. Investig Radiol. 2012;47(6):368–75.
8. Queiroz-Andrade M, Blasbalg R, Ortega CD, Rodstein MAM, Baroni RH, Rocha MS, Cerri GG. MR imaging findings of iron overload. Radiographics. 2009;29:1575–89.
9. Wood JC, Ghugre N. Magnetic resonance imaging assessment of excess iron in thalassemia, sickle cell disease and other iron overload diseases. Hemoglobin. 2008;32:85–96.
10. Cheon JE, Kim IO, Seo JK, Ko JS, Lee JM, Shin CI, Kim WS, Yeon KM. Clinical application of liver MR imaging in Wilson's disease. Korean J Radiol. 2010;11(6):665–72.
11. Ros PR, Sobin LH. Amyloidosis: the same cat, with different stripes. Radiology. 1994;190:14–5.
12. Marmoloya G, Karlins NL, Petrelli M, McCullough A. Unusual computed tomography findings in hepatic amyloidosis. Clin Imaging. 1990;14:248.
13. Bachler P, Baladron MJ, Menias C, Beddings I, Loch R, Zalaquett E, et al. Multimodality imaging of liver infections: differential diagnosis and potential pitfalls. Radiographics. 2016;36(4):1001–23.
14. Erturk SM, Yapici O. Liver inflammatory and infectious diseases. In: Hamm B, Ros PR, editors. Abdominal imaging, vol. 68. Berlin: Springer; 2013. p. 1001–12. Volume II Sec. V.
15. Mortele KJ, Segatto E, Ros PR. The infected liver: radiologic-pathologic correlation. Radiographics. 2004;24:937–55.
16. Semelka RC, Kelekis NL, Sallah S, Worawattanakul S, Ascher SM. Hepatosplenic fungal disease: diagnostic accuracy and spectrum of appearances on MR imaging. AJR. 1997;169(5):1311–6.
17. Pastakia B, Shawker TH, Thaler M, O'Leary T, Pizzo PA. Hepatosplenic candidiasis: wheels within wheels. Radiology. 1988;166:417–44.
18. Ferreira A, Ramalho M, de Campos RO, Heredia V, Roque A, Vaidean G, Semelka RC. Hepatic sarcoidosis: MR appearances in patients with chronic liver disease. Magn Reson Imaging. 2013;31(3):432–8.
19. Palmucci S, Torrisi SE, Caltabiano DC, Puglisi S, Lentini V, Grassedonio E, et al. Clinical and radiological features of extra-pulmonary sarcoidosis: a pictorial essay. Insights Imaging. 2016;7(4):571–87.
20. Karaosmanoglu AD, Onur MR, Sahani DV, Tabari A, Karcaaltincaba M. Hepatobiliary tuberculosis: imaging findings. AJR Am J Roentgenol. 2016:1–11.
21. Monzawz S, Ohtomo K, Oba H, et al. Septa in the liver of patients with chronic hepatic Schistosomiasis japonica: MR appearance. AJR. 1994;162:1347–51.
22. Mortele KJ, Ros PR. MR imaging in chronic hepatitis and cirrhosis. Semin Ultrasound CT MR. 2002;23(1):79–100.
23. Danon O, Duval-Arnould M, Osman Z, et al. Hepatic and splenic involvement in cat-scratch disease: imaging features. Abdom Imaging. 2000;25:182–3.
24. Rappaport DC, Cumming WA, Ros PR. Disseminated hepatic and splenic lesions in cat-scratch disease: imaging features. AJR. 1991;156:1227–8.
25. Moore EH, Russell LA, Klein JS, et al. Bacillary angiomatosis in patients with AIDS: multiorgan imaging findings. Radiology. 1995;197:67–72.
26. Van Allen RJ, Katz MD, Johnson MB, Laine LA, Liu Y, Ralls PW. Uncomplicated amebic liver abscess: prospective evaluation of percutaneous therapeutic aspiration. Radiology. 1992;183:827–30.
27. Czermak BV, Akhan O, Hiemetzberger R, Zelger B, Vogel W, Jaschke W, et al. Echinococcosis of the liver. Abdom Imaging. 2008;33(2):133–43.
28. Kantarci M, Bayraktutan U, Karabulut N, Aydinli B, Ogul H, Yuce I, et al. Alveolar echinococcosis: spectrum of findings at cross-sectional imaging. Radiographics. 2012;32(7):2053–70.
29. Alghofaily KA, Saeedan MB, Aljohani IM, Alrasheed M, McWilliams S, Aldosary A, et al. Hepatic hydatid disease complications: review of imaging findings and clinical implications. Abdom Radiol (NY). 2017;42(1):199–210.
30. Boll DT, Merkle EM. Diffuse liver disease: strategies for hepatic CT and MR imaging. Radiographics. 2009;29:1591–614.

Open Access This chapter is licensed under the terms of the Creative Commons Attribution 4.0 International License (http://creativecommons.org/licenses/by/4.0/), which permits use, sharing, adaptation, distribution and reproduction in any medium or format, as long as you give appropriate credit to the original author(s) and the source, provide a link to the Creative Commons license and indicate if changes were made.

The images or other third party material in this book are included in the book's Creative Commons license, unless indicated otherwise in a credit line to the material. If material is not included in the book's Creative Commons license and your intended use is not permitted by statutory regulation or exceeds the permitted use, you will need to obtain permission directly from the copyright holder.